CHAPTER-6

REACTION FORCE TIME CURVE AND IMPACT AREA

6.1 GENERAL

The reaction force time response curve of aircraft is widely used as the loading function to evaluate the response of any NPP structure. In the present chapter the effect of target curvature, deformability and impact angle has been taken in to account in order to evaluate the reaction-time response of the aircraft. The Boeing 707-320 has been considered to validate the results with existing results. The reaction time curve obtained against deformable target has been found to be lesser than rigid target of size. The response of containment building has been studied against the geometric model of aircraft, reaction time curve and trifurcation approach. The response of containment against the geometric model of aircraft has been found to be very close to that obtained against the reaction time curve used with area trifurcation scheme.

6.2 REACTION FORCE-TIME CURVE

When an aircraft is impacted on a target, the reaction force is produced. The reaction force curve with respect to time is called reaction force time history curve. The calculation of the reaction-time curve by aircraft impact on a target is very complex phenomenon. A rigid and a deformable target has been taken into consideration to get the actual reaction force time curve. Riera (1968) proposed a reaction force time curve on flat rigid target for normal impact of Boeing 707-320 aircraft. In In actual scenario, the

targets are deformable. The impact angle on the target may not be normal and the target may not be flat, so reaction force time response curve must be modified.

In the present study, it is focused to reevaluate the reaction force time response curve for Boeing 707-320 aircraft for three different parameters. The parameters are

- Effect of target curvature
- Effect of target deformability
- Effect of aircraft impact angle

6.2.1 Effect of target curvature

To study the effect of target curvature, the geometric model of aircraft has been crashed against non-deformable curved targets with different radius i.e., 30 m, 40m, 50m and infinity as shown in Fig. 6.1. The impact velocity of Boeing 707-320 aircraft has been considered as 103m/sec against the non-deformable rigid target. To find out proper reaction force time curve on rigid target, mass distribution of aircraft model along longitudinal as well as transverse direction must be considered which has been obtained by using the concept of Riera (1968), Fig. 6.2. The plan view of target with different radii under Boeing 707-320 aircraft impact has been shown in Fig. 6.3.

Figs. 6.4 and 6.5 are showing the impact force and impulse-time history curves for aircraft impact on the containment with different radius, respectively. For the impact of Boeing 707-320 aircraft, the maximum impact force has been found to be 400 MN for target with 50m radius at time 0.17 sec, 330 MN for the target with 40m radius at 0.175 sec and 280 MN for the target with 30m radius at time 0.18 sec (Fig. 6.4). However, against the non-deformable flat target the maximum impact force has been found to be

470 MN at 0.16 sec. Therefore, as the curvature of the target is decreased the peak impact force is increased while the time of its arrival has decreased. This is due to the fact that in case of flat target the main component of reaction is in the normal direction to the target surface opposite to the applied force, while the other two directional components are negligible. However, when the curvature is introduced in the target geometry, these two components of reaction have also developed which become prominent with an increase in curvature. For Boeing 707-320 aircraft the peak impact force has been found to decrease by 40% for the 30m radius target as compared to flat target. Hence, it may be concluded that effect of target curvature cannot be neglected while obtaining the reaction time curve for the aircraft. It may also be concluded that the acceptance of the reaction curve obtained against flat target as the design load will result in the overestimation of the resultant design parameters.

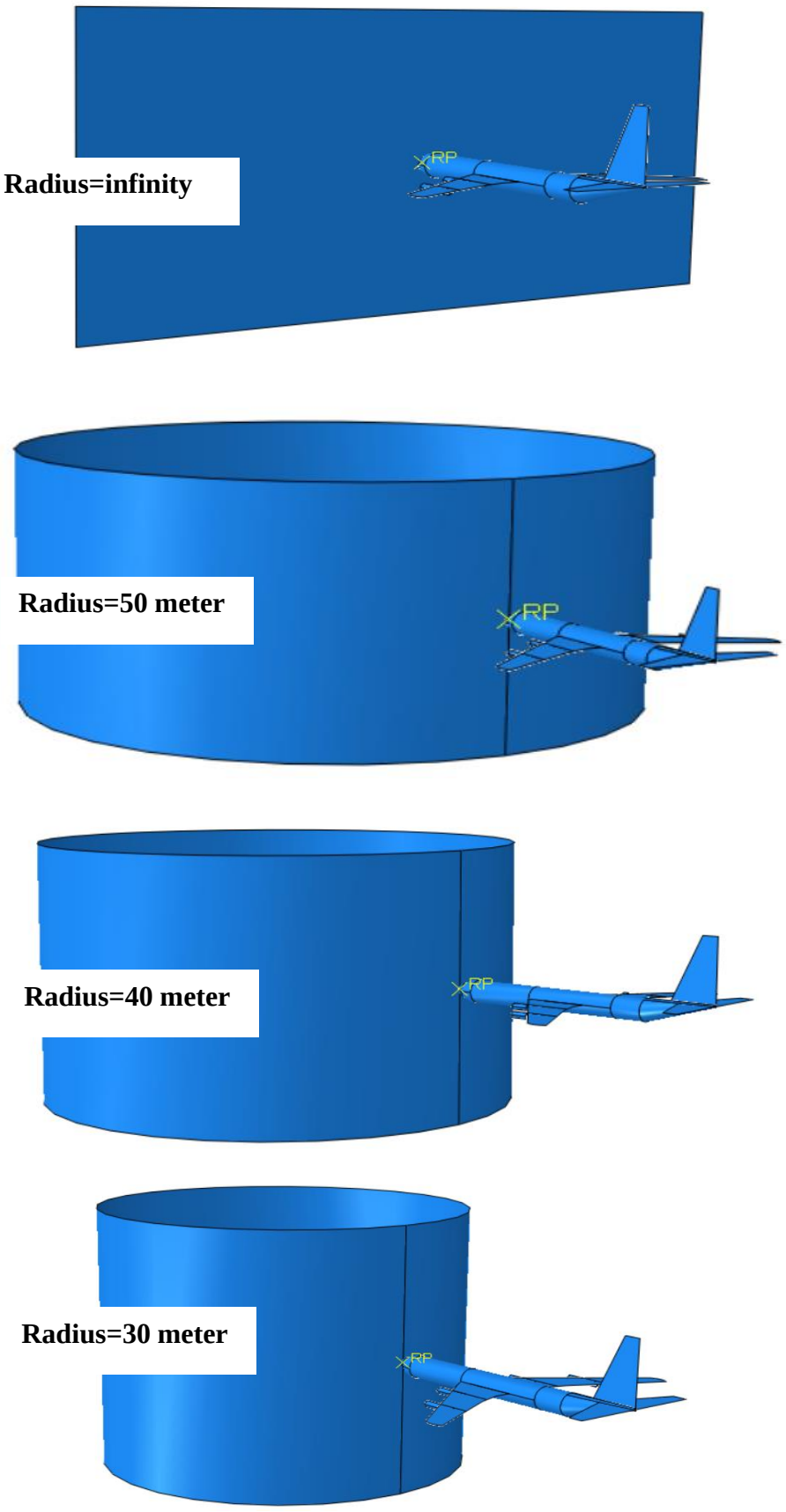

Fig. 6.1 Impact of Boeing 707-320 aircraft on target with different radius.

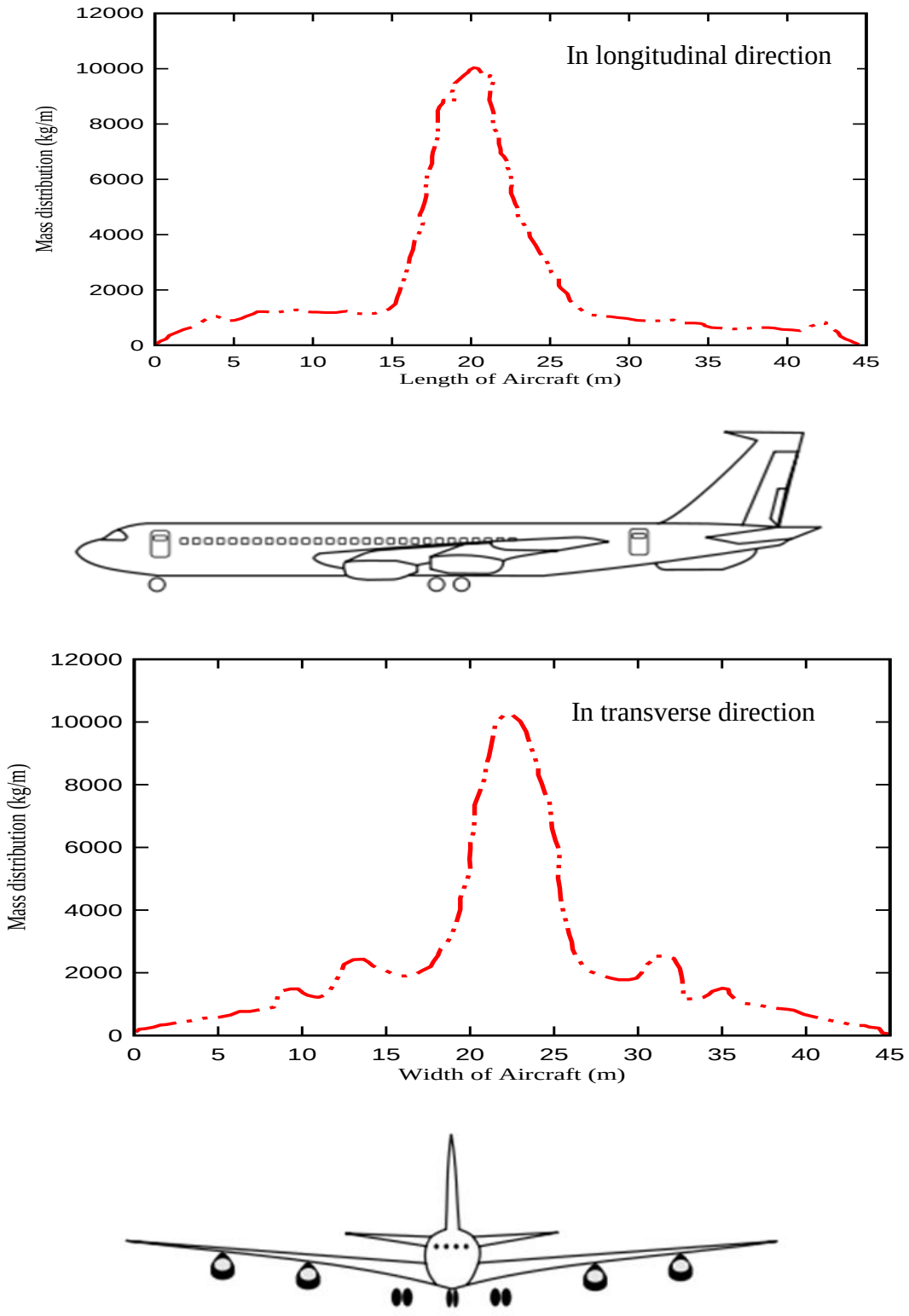

Fig. 6.2 Transverse mass distribution of Boeing 707-320 aircraft.

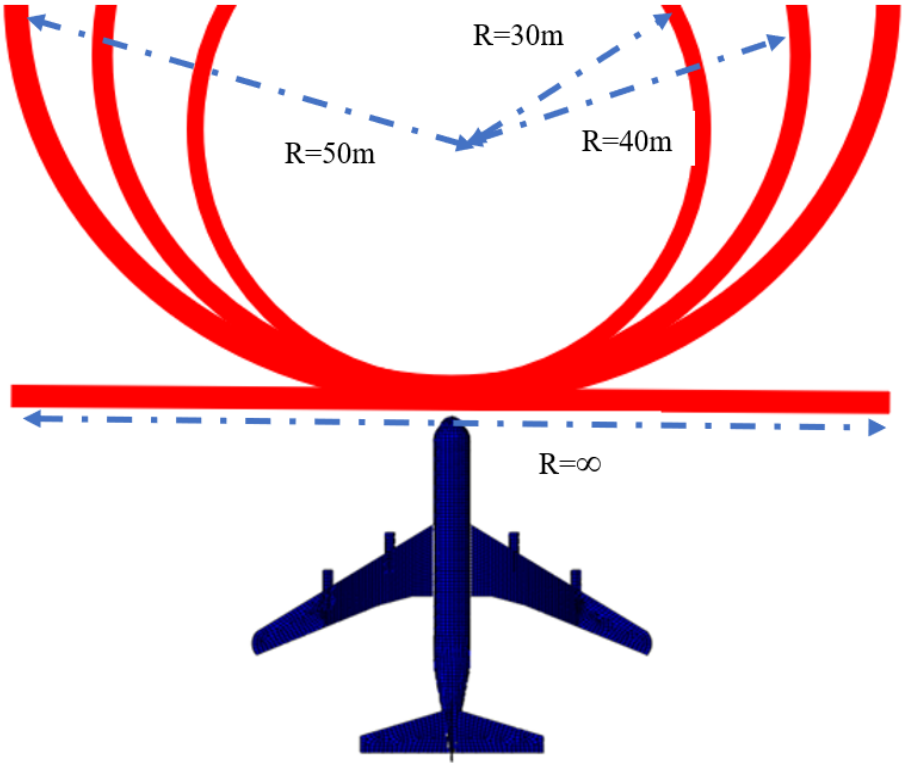

Fig. 6.3 Plan view of Boeing 707-320 aircraft with different target

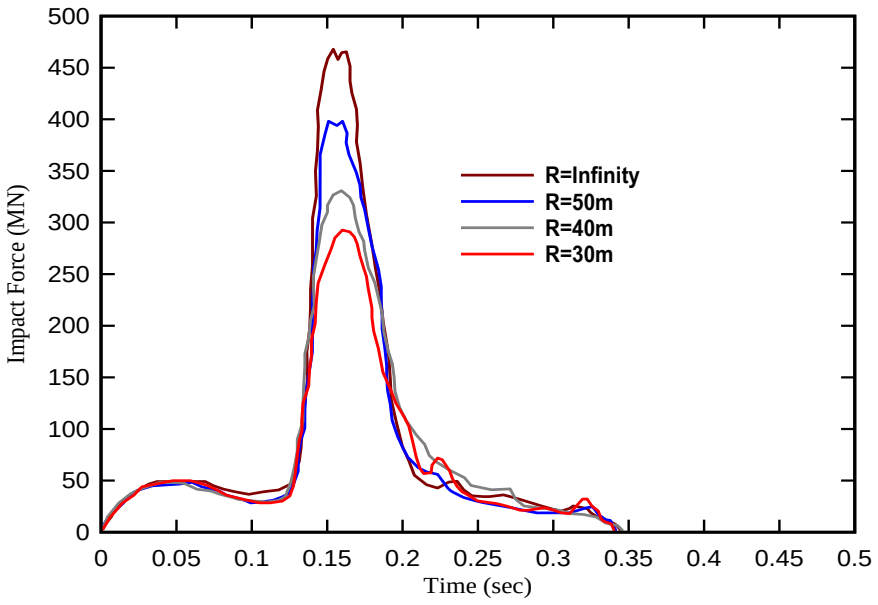

Fig. 6.4 Impact force–time response of target with different radius.

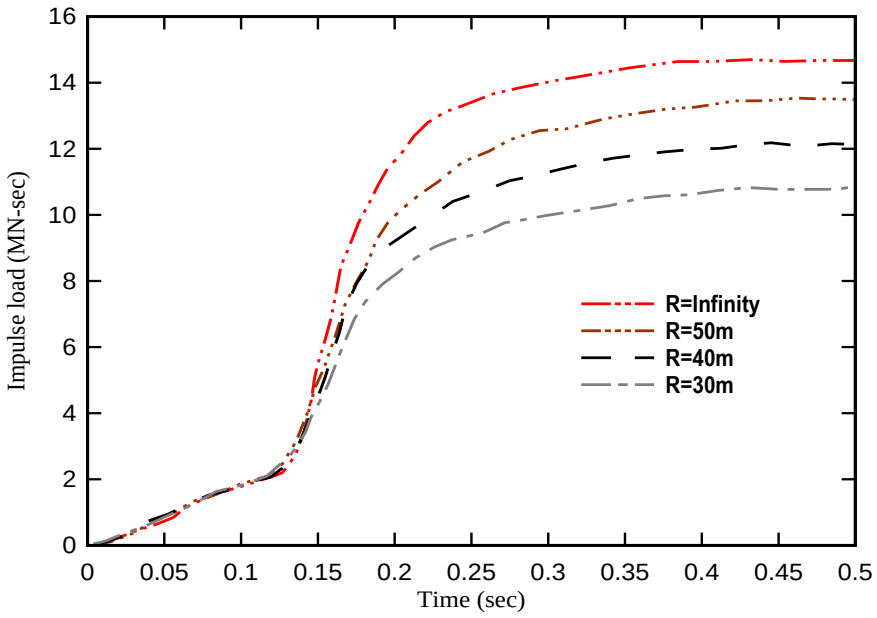

Fig. 6.5 Impulse–time response of target with different radius.

6.2.2 EFFECT OF TARGET DEFORMABILITY

In order to evaluate the influence of target flexibility, two flat plates have been taken into consideration. One plate is rigid and another plate is deformable, Fig. 6.6. Here the impact location is kept at the middle height of the plate. The size of plate deformable plate 100m X 50m with thickness 1.2m is considered. At the boundary of plate, fixed support is used.

The reaction-time curve thus obtained has been compared with that obtained against the non-deformable target. A significant downfall in the peak impact force has been noticed in case of the deformable target for the impact of Boeing 707-320 aircraft, see Fig. 6.7. The peak impact force against deformable target has been found to decrease by 45% for Boeing 707-320 aircraft. The reduction in reaction force against the containment structure is due to the fact that some energy has been dissipated in the

deformation of the structure. Thus, the net reaction obtained is lesser than that obtained against non-deformable target of same diameter. Hence, it may be concluded that the reaction time response curve is a function of the stiffness of the target.

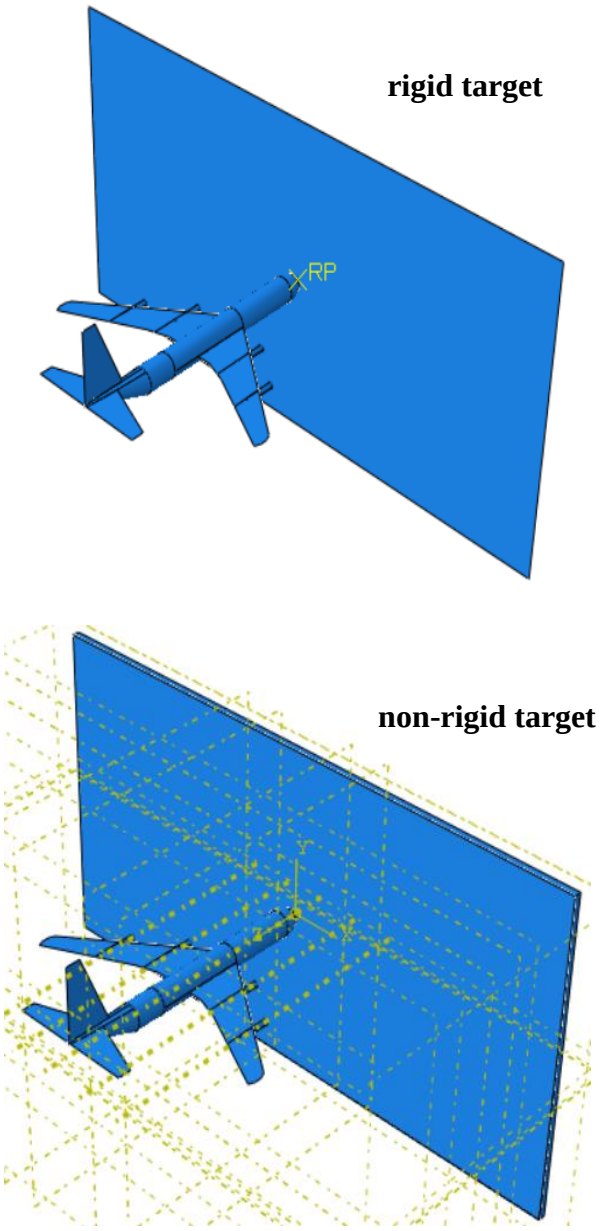

Fig. 6.6 Boeing 707-320 model on rigid target and non-rigid target.

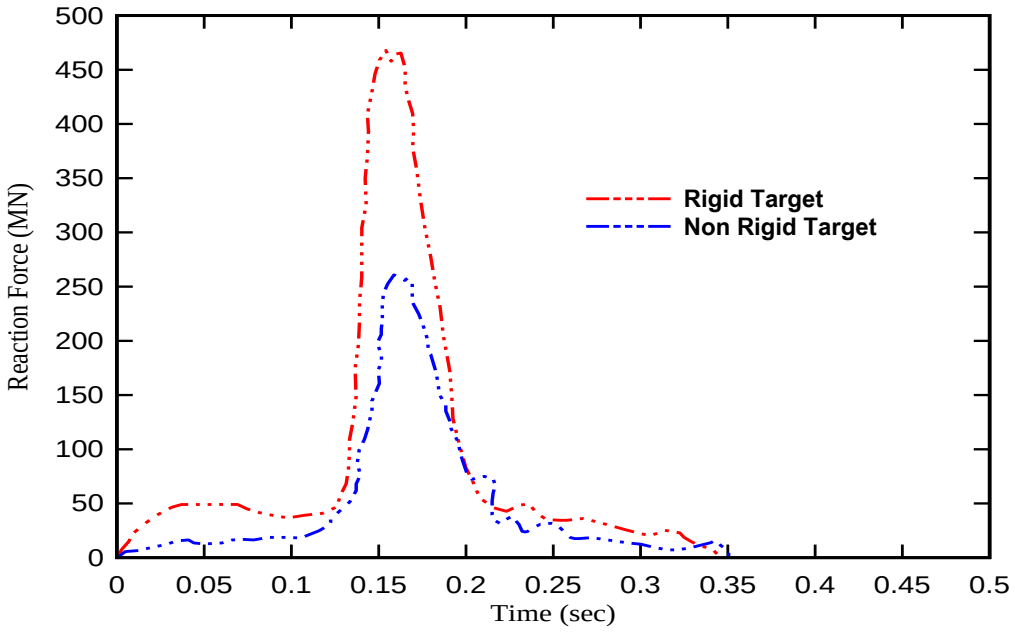

Fig. 6.7 Reaction force–time response of rigid and non-rigid target.

6.2.3 EFFECT OF AIRCRAFT IMPACT ANGLE

The angle of aircraft impact may not be normal to the target so the evaluation of reaction time response curve for different impact angles must be investigated. The angles of impact 0^o, 20^o, 30^o, 45^o, 60^o and 75^o with horizontal are considered, Fig .6.8. When reaction force vs time graphs have been plotted for these impact angles, 0-degree impact angle is responsible for maximum reaction force. When the angle increases with horizontal, the reaction force deceases, Fig. 6.9. So, the impact normal to the target is most critical. The formulation of reaction time response curve for 0-degree impact which was given by Riera,1968 need not further improvement for other impact angles because the case should be studied for maximum response. The formulation must be modified for any other impact angles except 0^o if required.

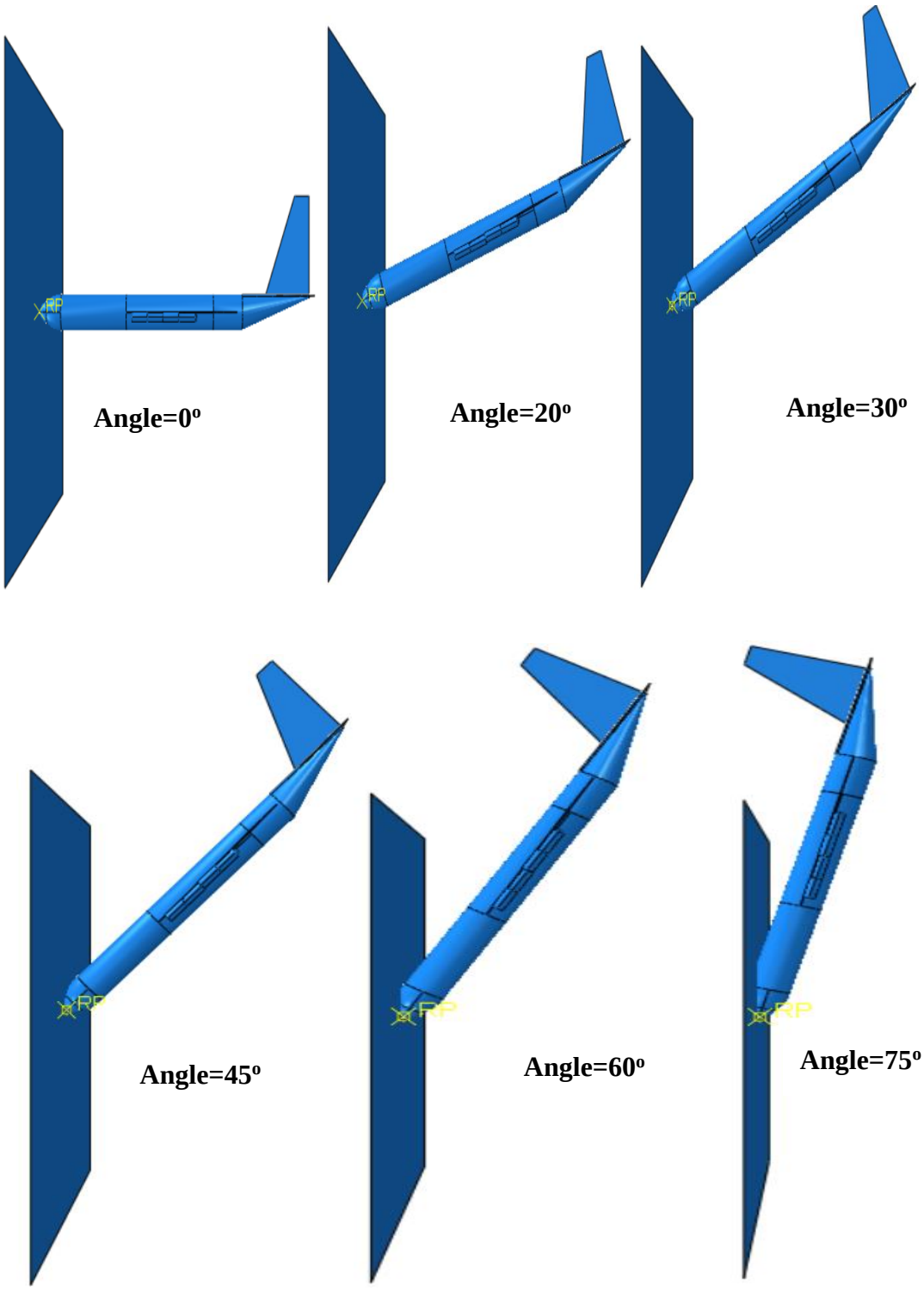

Fig. 6.8 Boeing 707-320 model on rigid target with different impact angle.

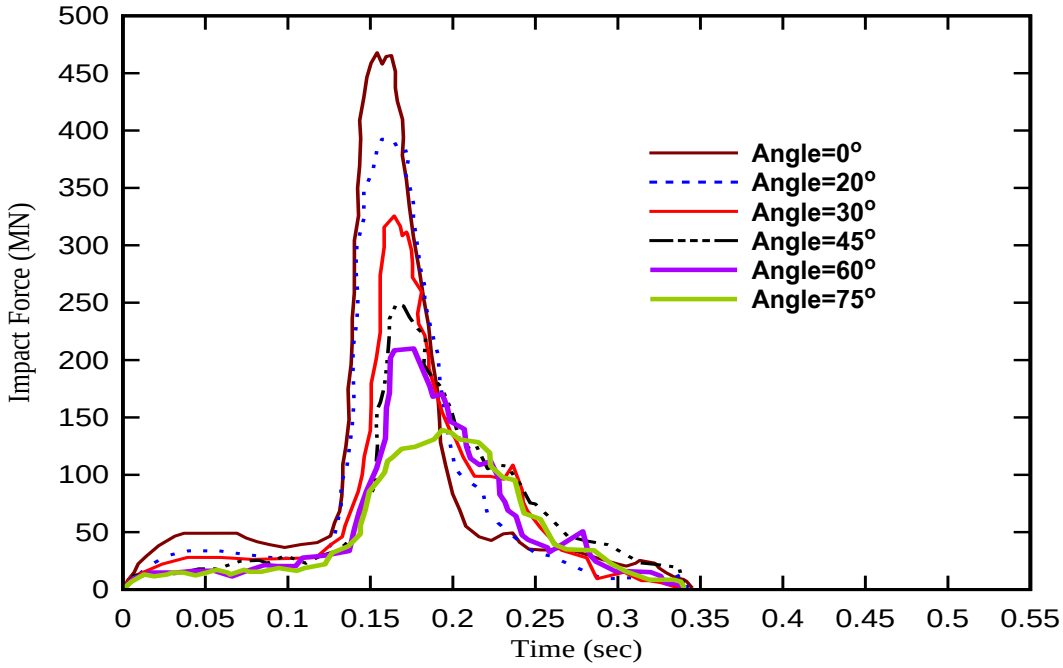

Fig. 6.9 Impact force–time response of target with different impact angle.

6.3 CALCULATION OF EFFECTIVE AREA UNDER IMPACT

In order to evaluate the containment response through the reaction-time approach, the area of impact for the application of load is highly important. A smaller area will increase the intensity of the pressure and hence the response will be localized and overestimated, while a larger area will reduce the deformations and hence underestimate the response. The impact area of an aircraft can not be constant. It is a function of time because the cross-sectional area of aircraft varies with the length of aircraft. In maximum number of available literatures, the average contact area of the of aircraft has been considered as the impact area.

Determination of actual impact area is very complex. An effort has been made to modify the area of impact. The numerical approach has been employed to evaluate the actual impact area which is a function of time. The crushed profile of Boeing 707-320 aircraft against non-deformable flat target has been studied at different time interval, see Fig. 6.10. It is possible to evaluate of impact area with respect to time through the numerical simulation. Abbas (1992) plotted the variation of impact load for Boeing 707-320 with respect to distance from the nose of aircraft. With the help of these data an effective cross-sectional area verses time graph of Boeing 707-320 has been plotted for the impact velocity 103 m/s, Fig. 6.11. However, it has been reported by Yang and Godfrey (1970) that the contact area between the aircraft and target increases by 10 to 15% as compared to the actual cross-sectional area of aircraft. Therefore, the cross-sectional area calculated above was increased by 15% to obtain the contact area for Boeing 707-320 aircraft.

The contact area versus-time curve thus obtained has been found to have close correlation with that of the curve proposed by Riera (1968), Fig. 6.11. In all these curves, initially sharp rise is due to the crushing of nose of the aircraft which is comparatively stiffer. There is again a steep rise in the contact area as soon as the wings come in contact. The tail of the aircraft generally not come in the contact particularly during the normal impact due to the fact that the crushed body of the aircraft restricts the contact of the tail with that of the containment. Hence, the contact area becomes constant once the complete wings come in the contact. The average area calculated from Riera (1968) curve is 28.25 m^2 while that obtained from the present investigation is 28.0 m^2 through numerical approach, Fig. 6.11. It has also been noticed from Fig. 6.11 that the maximum contact area from all the studies is approximately equivalent to 40 m^2.

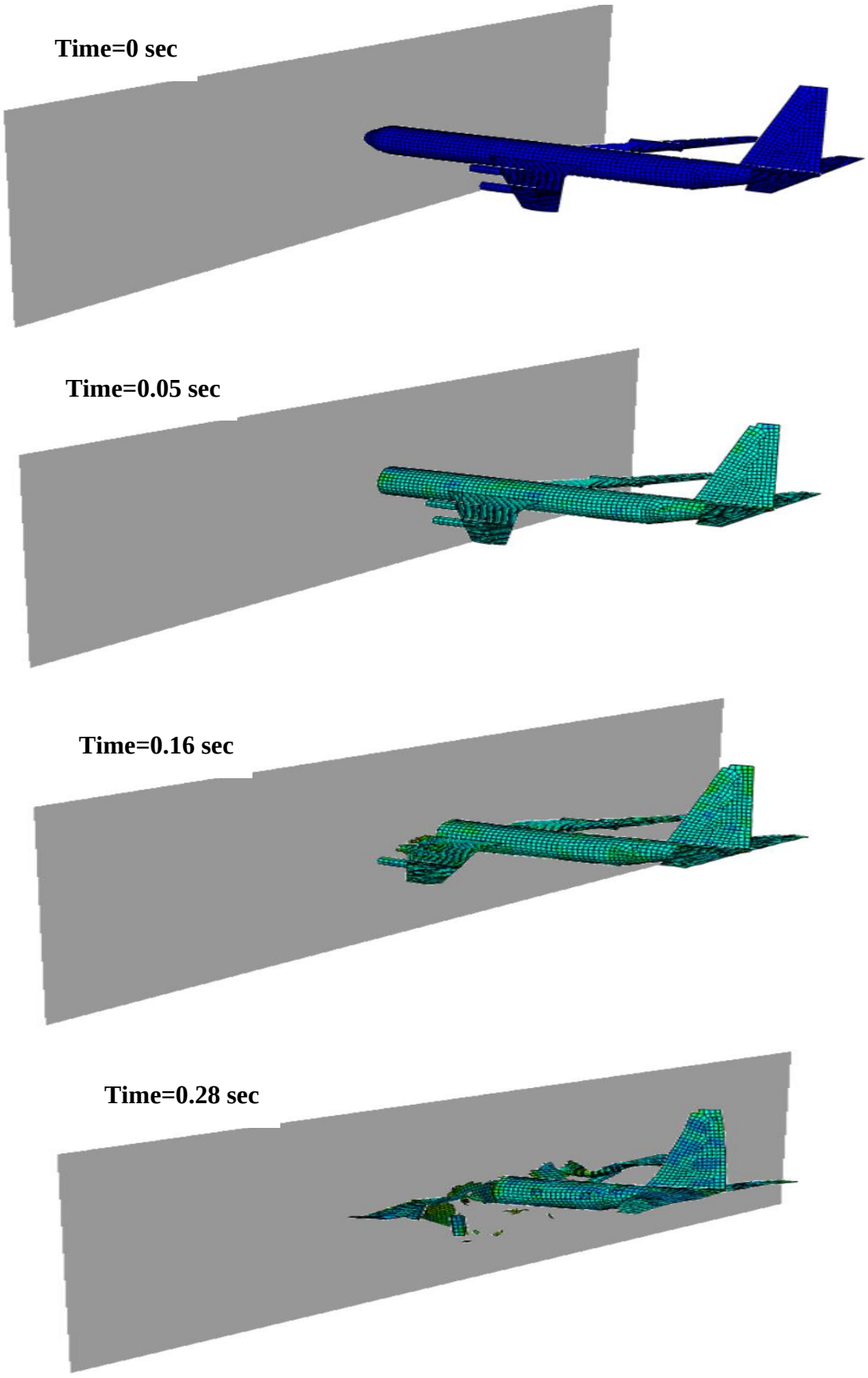

Fig. 6.10 Crushing behaviour of Boeing 707-320 at different time interval

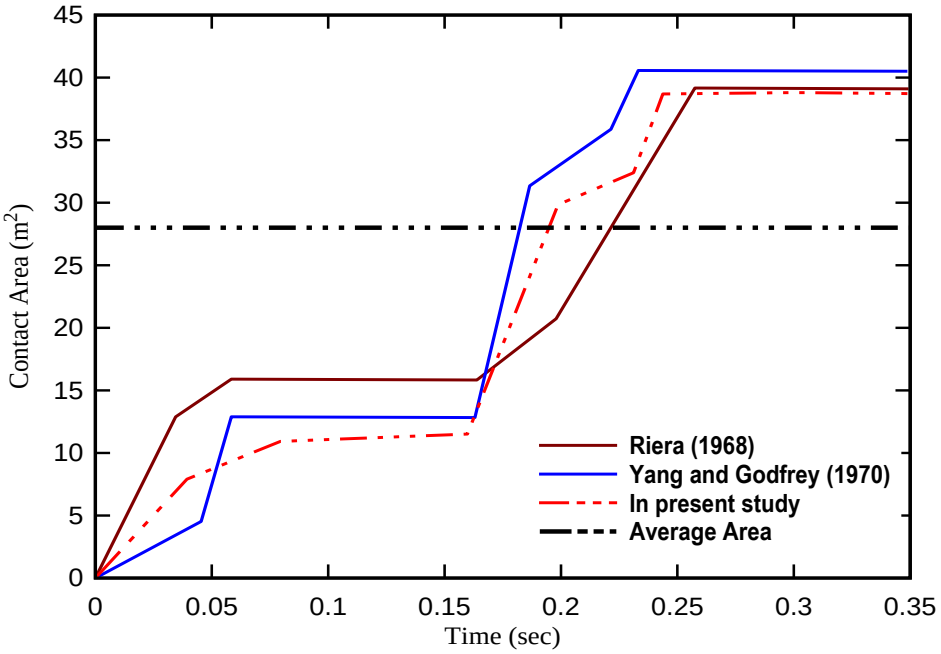

Fig. 6.11 Contact area of Boeing 707-320 aircraft through different methods

6.4 NPP CONTAINMENT WALL UNDER REACTION TIME CURVE AND GEOMETRIC MODEL

A comparative study of the response of containment has been performed adopting different loading approaches. The aircraft crash on the TMIR containment has been simulated through the geometric model as well as reaction-time curve.

However, impact force has been applied on the containment using two different approaches. In the first approach, the area of application has been considered to be the average of the total contact area given in Fig. 6.12 for Boeing 707-320. The respective reaction-time curve has been applied as a function of time over the average area assumed to be of circular shape. In the second approach whole geometric mode of Boeing 707-320 aircraft has been applied on TMIR containment wall, Fig. 6.12.

Hence, the response of the containment in the present study has been studied through two independent approaches;

(i) Average area approach for the application of reaction-time curve

(ii) The geometric model of aircraft impacted on the containment

It should be noted that through each of the above approach the aircraft has been considered to hit the containment at its mid height, 27.25m from the base. The results obtained have been compared and discussed. The tension damages in the containment, at the center of the impact location has been shown in Fig. 6.13. Against Boeing 707-320 aircraft, a maximum displacement/deformation in concrete body has been found to be 0.0149m and 0.0624m through average area approach and through the geometrical model of aircraft respectively, Fig. 6.14. Similarly, the maximum displacement/deformation in the steel reinforcement has been found to be 0.0148m and 0.0591m under average area approach and through the geometric model of aircraft respectively, Fig. 6.15. Fig. 6. 16 is showing the deformation in inner steel liner and that is 0.0144m for average area approach and 0.0586m for geometric model. Further, the deformation predicted by the average area method has been found to be very low compared to geometric model of aircraft.

For Boeing 747-400 aircraft, the axial stress variation in the outer set of reinforcement is shown in Fig. 5.30. The maximum stress has been found to be 8.5 MPa, 36.9 MPa and 62.9 MPa in concrete, steel reinforcement and inner steel liner respectively for average area approach, Fig. 6.17-6.19. Similarly, the maximum stress has been

noticed to be 34.2 MPa, 163 MPa and 306 MPa in concrete, steel reinforcement and inner steel liner respectively for geometric model impact, Fig. 6.17-6.19.

To get the global behaviour of containment two paths A and B has been taken which is shown in Fig. 6.20. Both the paths are at the inner face of the concrete body. The path A is along the height whereas path B is along the periphery of containment. Figs. 6.21-6.24 are showing the deformation and stress variation along path A and B. From these plots it is observed that deformation and stress for geometric model approach is much higher than average area approach.

The deformation of a node at the center of impact has also been plotted in Fig. 6.25. It has been noticed that the displacement in the impact region increases with an increase in the loading. However, as the load is reduced the elastic recovery of the target has been found to occur due to which the final displacement is significantly reduced, Fig. 6.25. The elastic recovery has been found to be very significant corresponding to the geometric model. Against the impact of average area approach however, elastic recovery was found to be insignificant, Fig. 6.25. It has also been noticed that the stress in the impact region increases with an increase in the loading and then deceases, Fig. 6.26.

It may be concluded from the above results that stresses developed in the concrete as well reinforcement is within the permissible limit. The geometrical model occurred very high deformations in the containment.

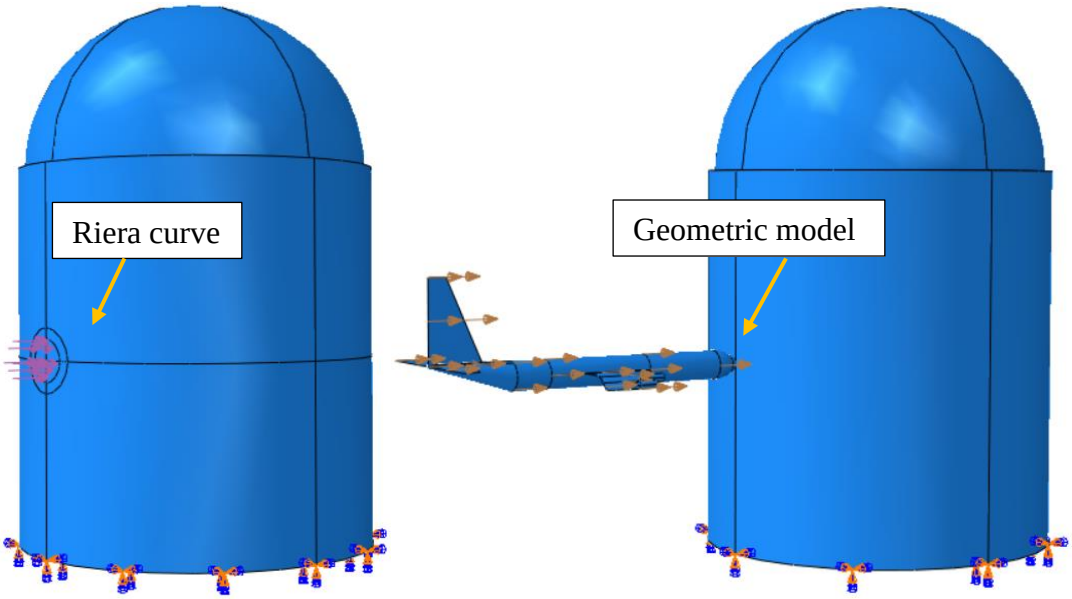

Fig. 6.12 Three-mile island containment subjected to Riera force time history curve and geometric model of Boeing 707-320 aircraft

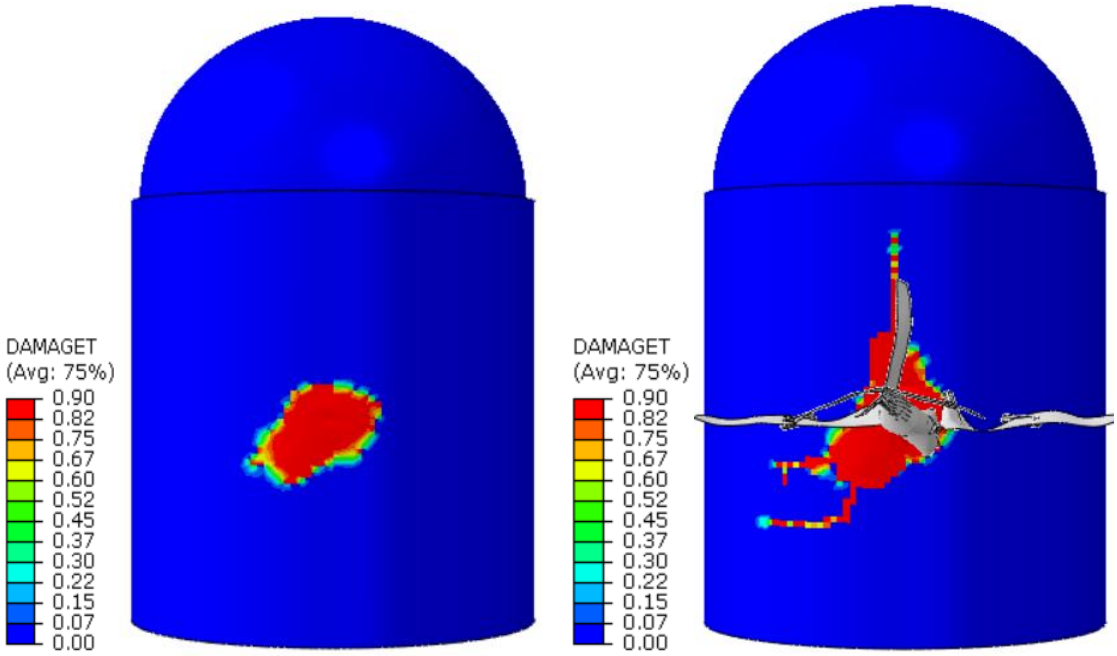

Fig. 6.13 Tension damage profile in concrete using (a) Riera curve (b) Geometric model

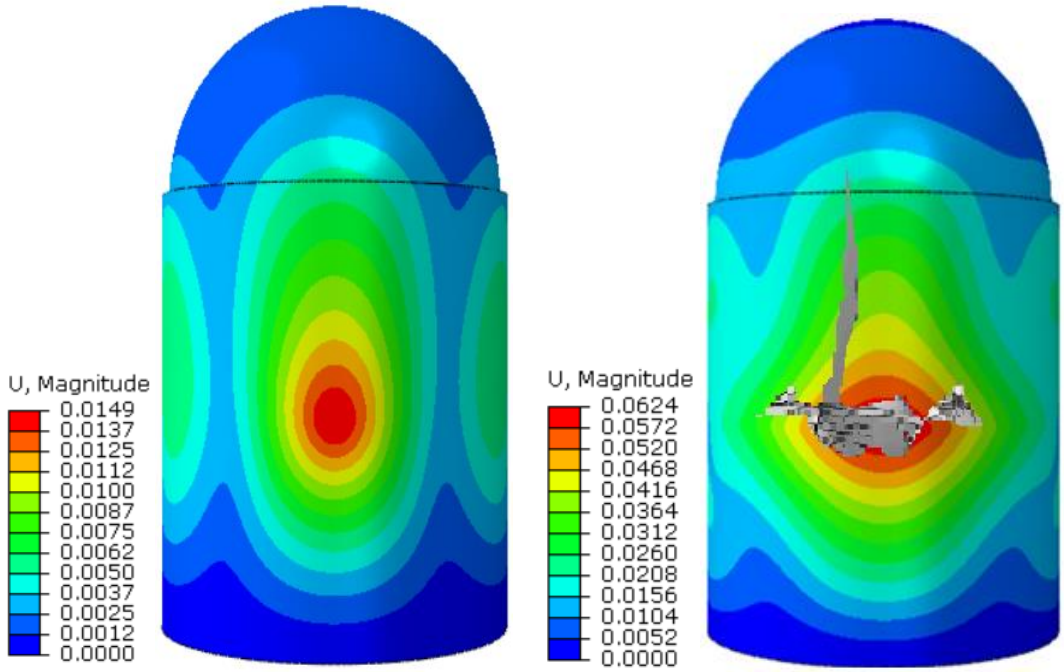

Fig. 6.14 Deformation profile in concrete using (a) Riera curve (b) Geometric model

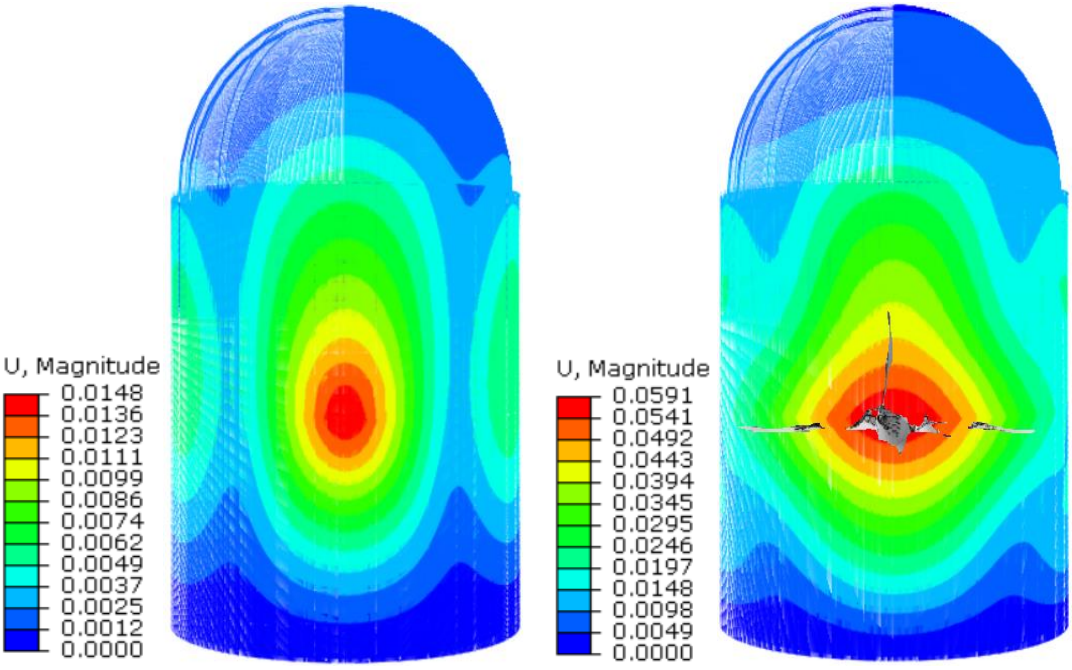

Fig. 6.15 Deformation profile in steel reinforcement using (a) Riera curve (b) Geometric model

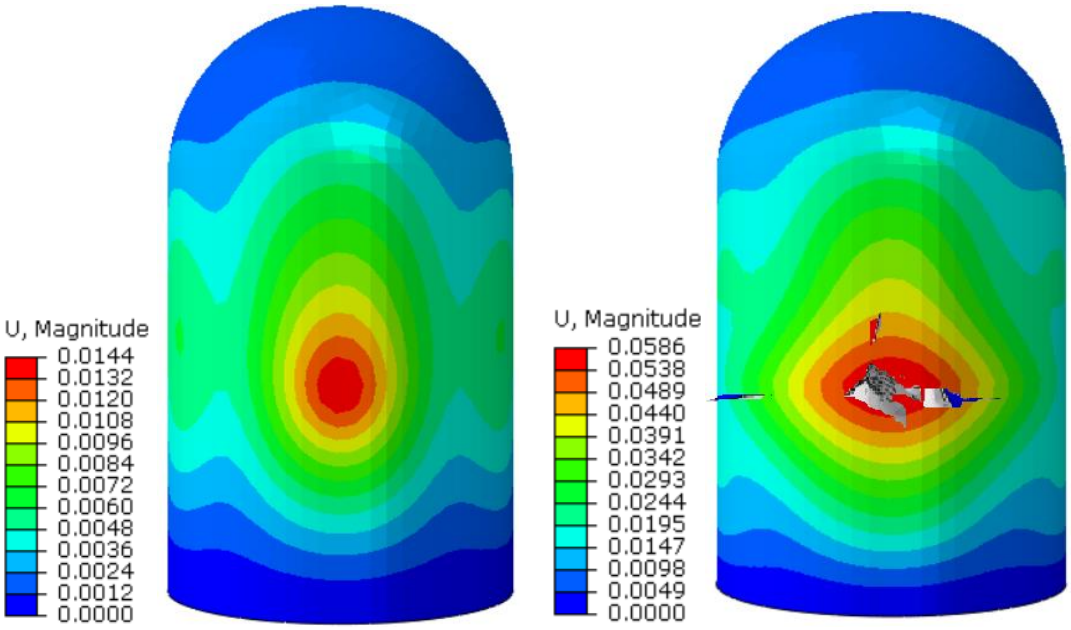

Fig. 6.16 Deformation profile in inner steel liner using (a) Riera curve (b) Geometric model

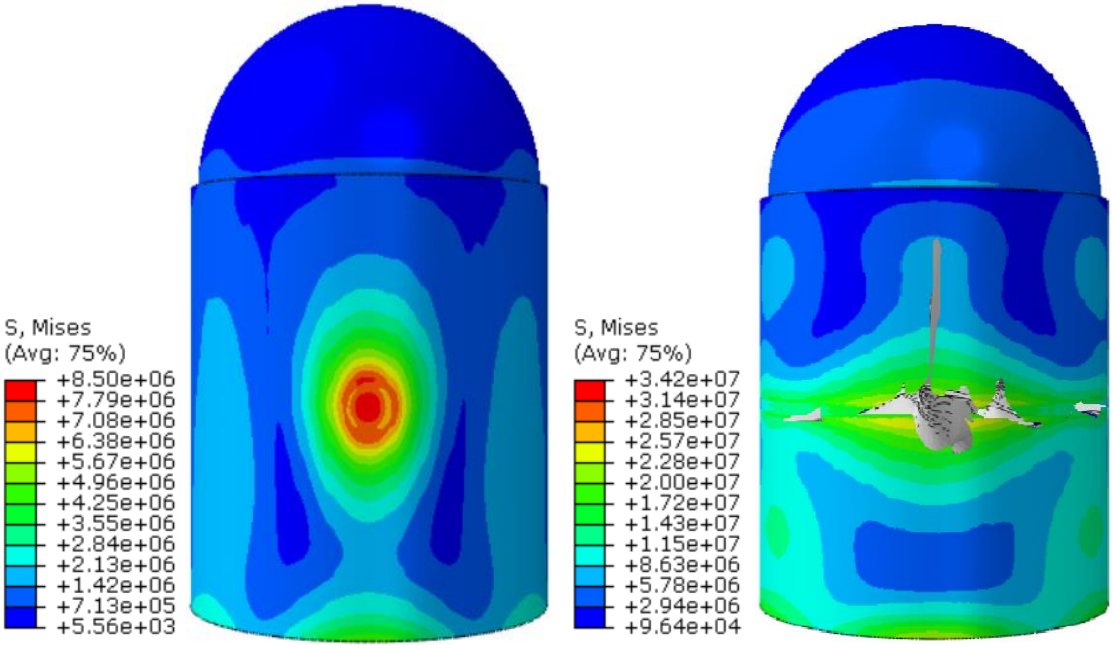

Fig. 6.17 Stress profile in concrete using (a) Riera curve (b) Geometric model

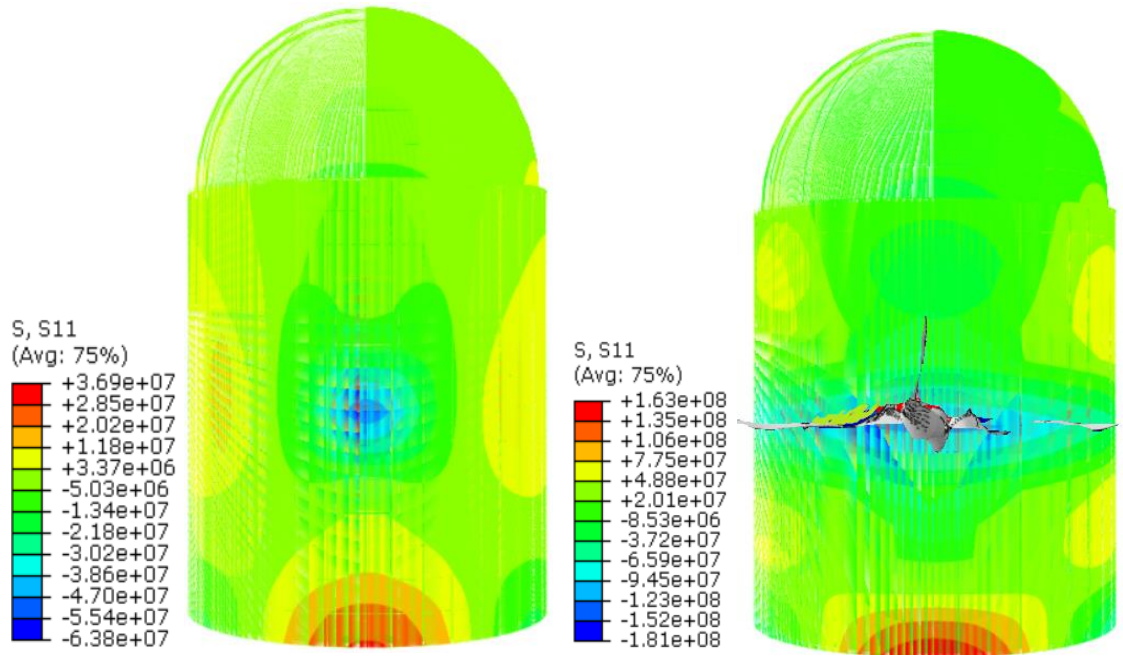

Fig. 6.18 Stress profile in steel reinforcement using (a) Riera curve (b) Geometric model

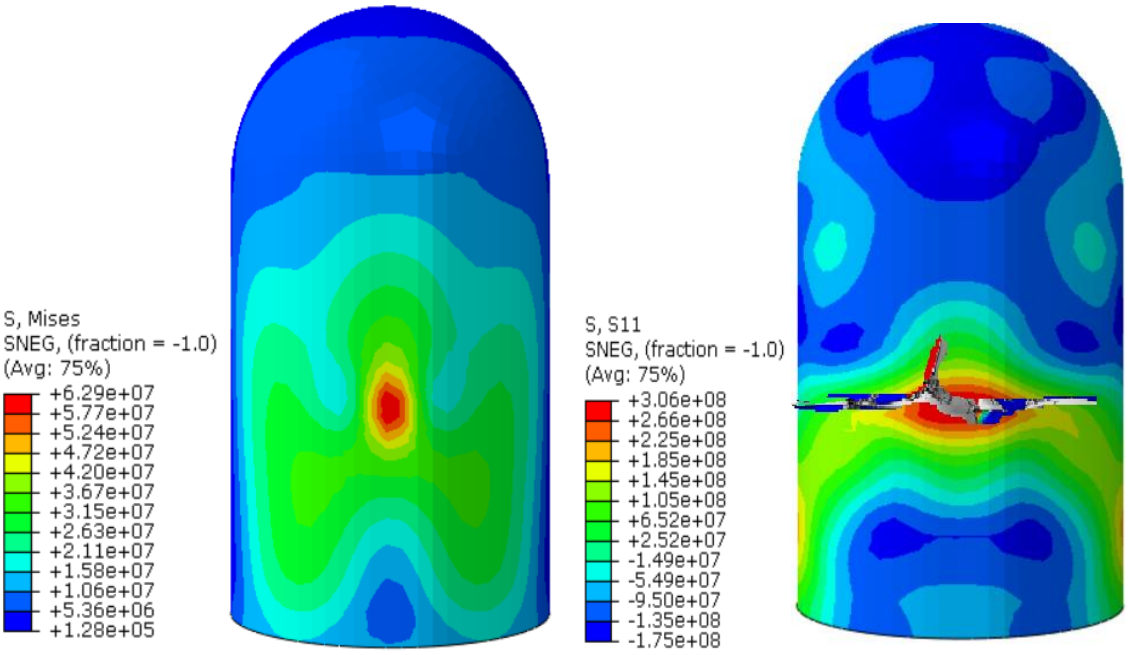

Fig. 6.19 Stress profile in inner steel liner using (a) Riera curve (b) Geometric model

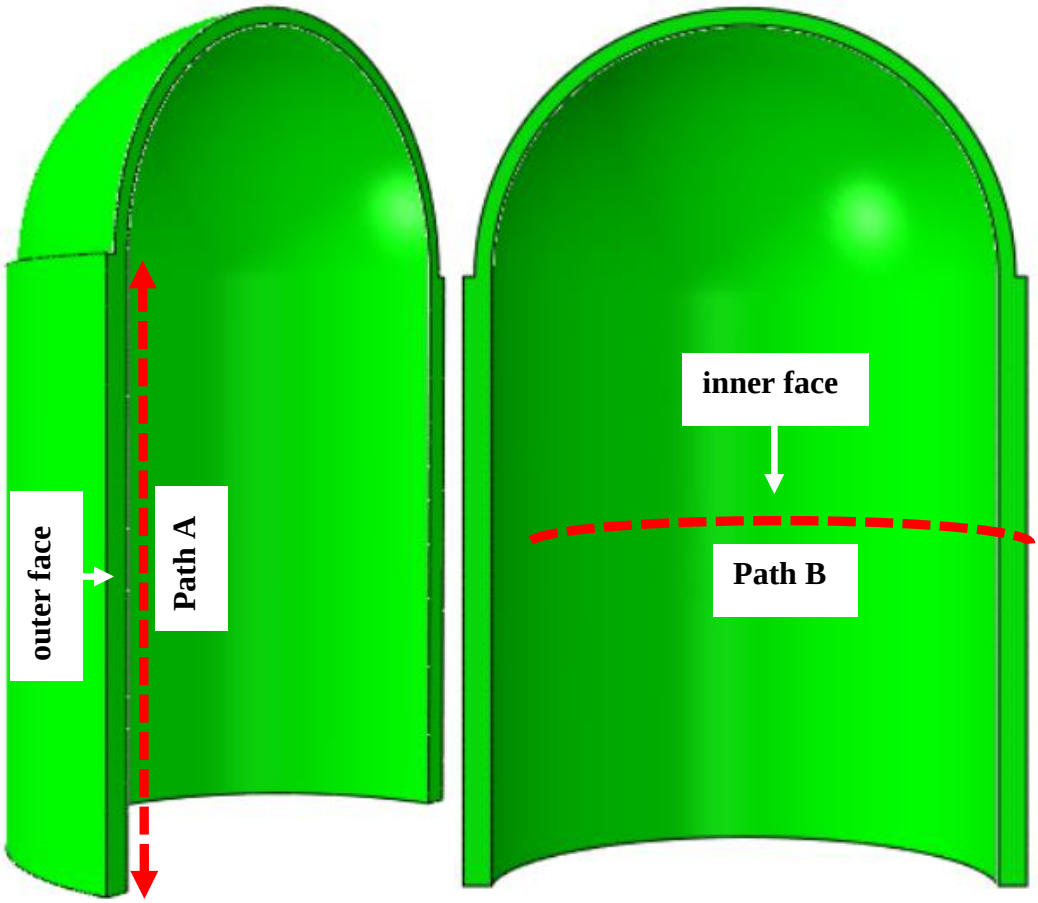

Fig. 6.20 Three-mile island containment with different paths for plotting results

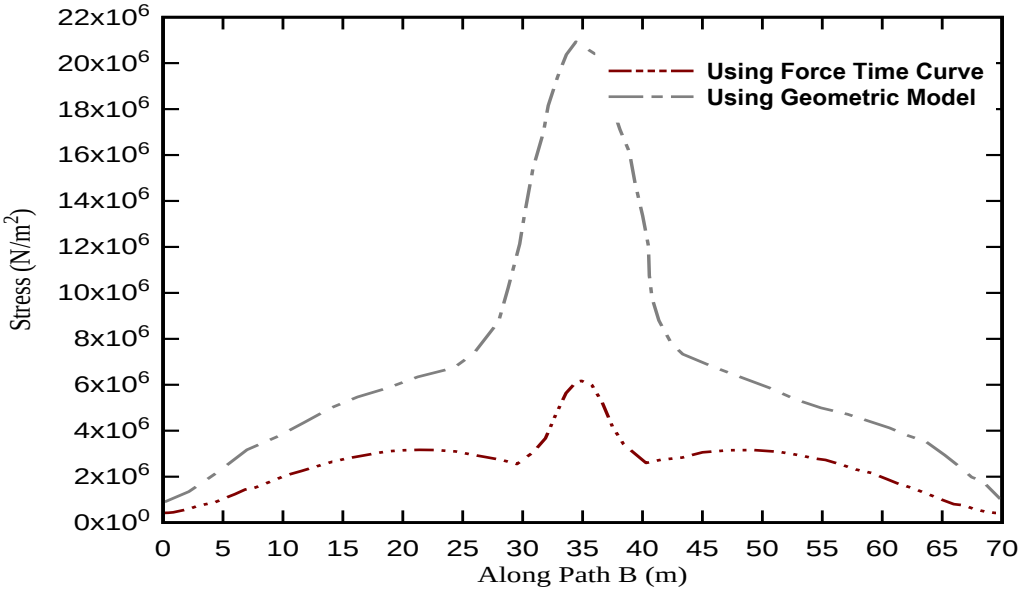

Fig. 6.21 Deformation in concrete along path-B using different method

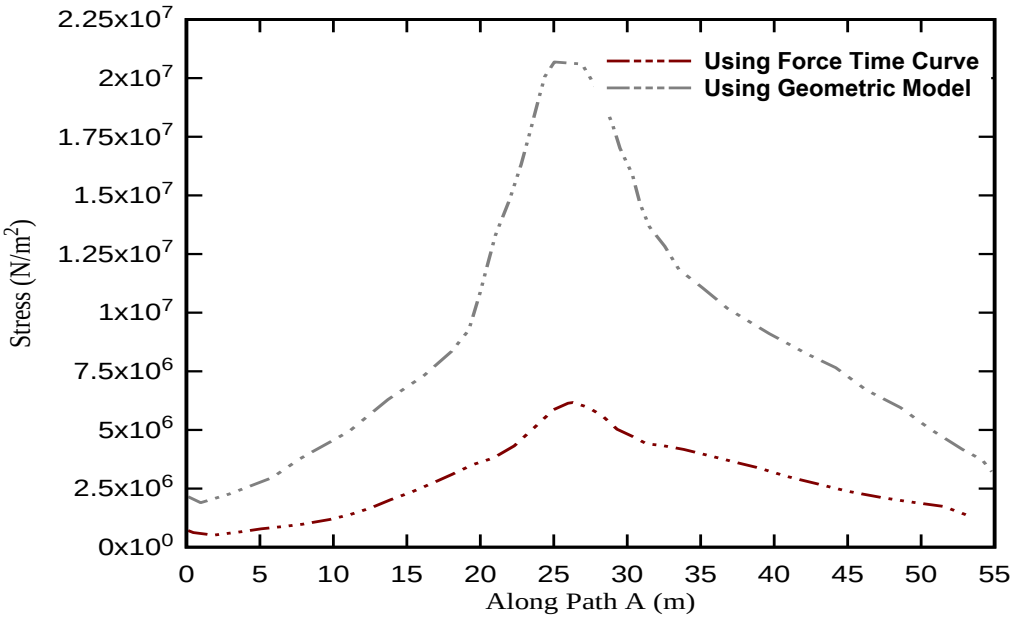

Fig. 6.22 Deformation in concrete along path-A using different method

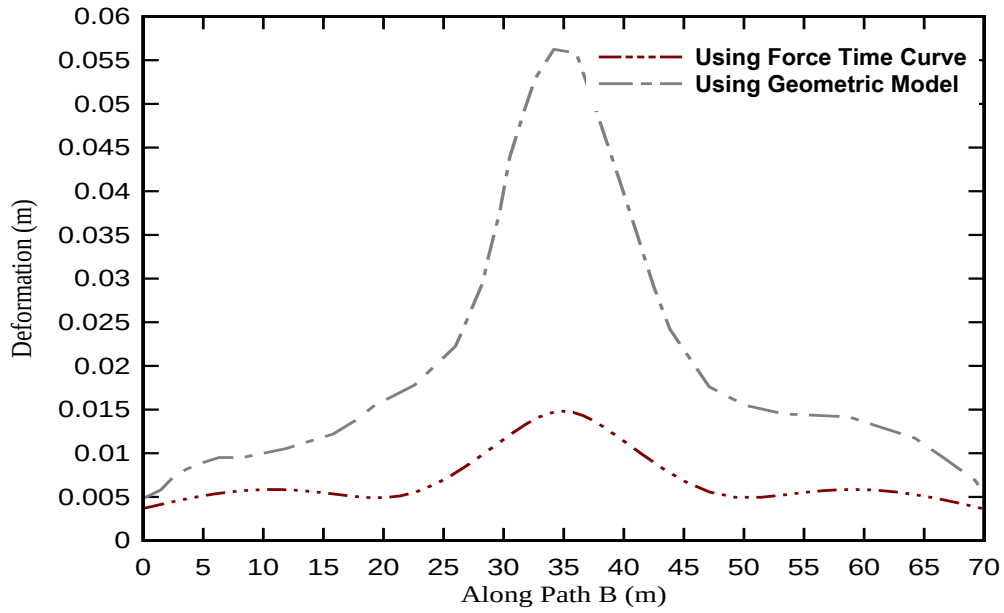

Fig. 6.23 Stress in concrete along path-B using different method

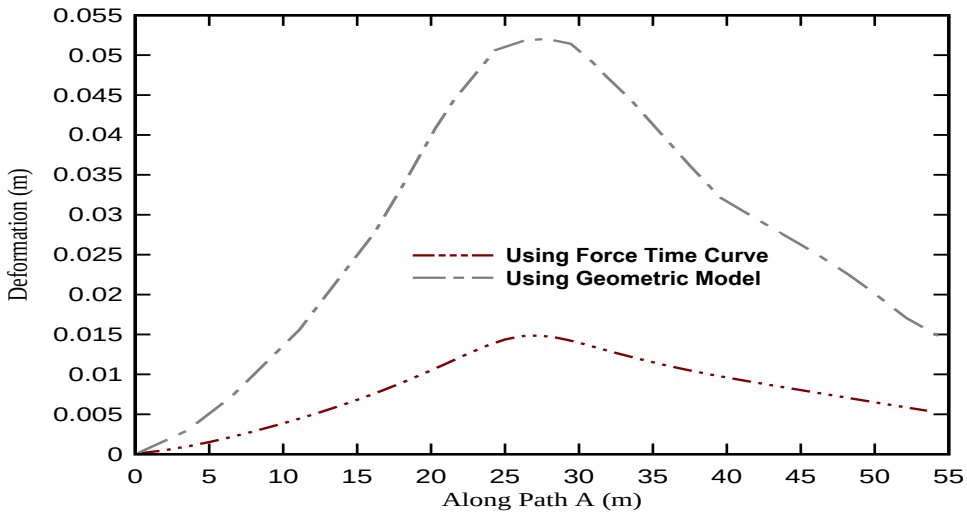

Fig. 6.24 Stress in concrete along path-A using different method

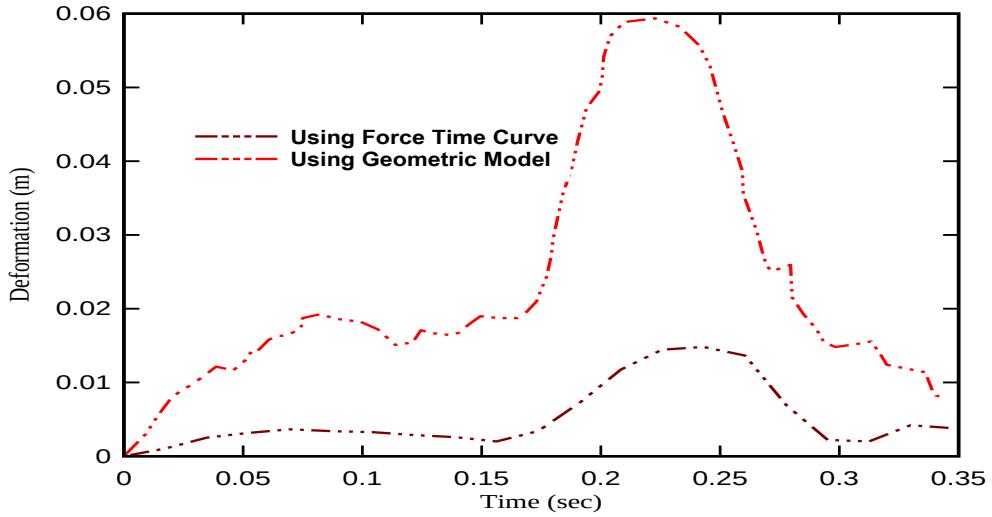

Fig. 6.25 Deformation in single element at impact location of concrete body using different method

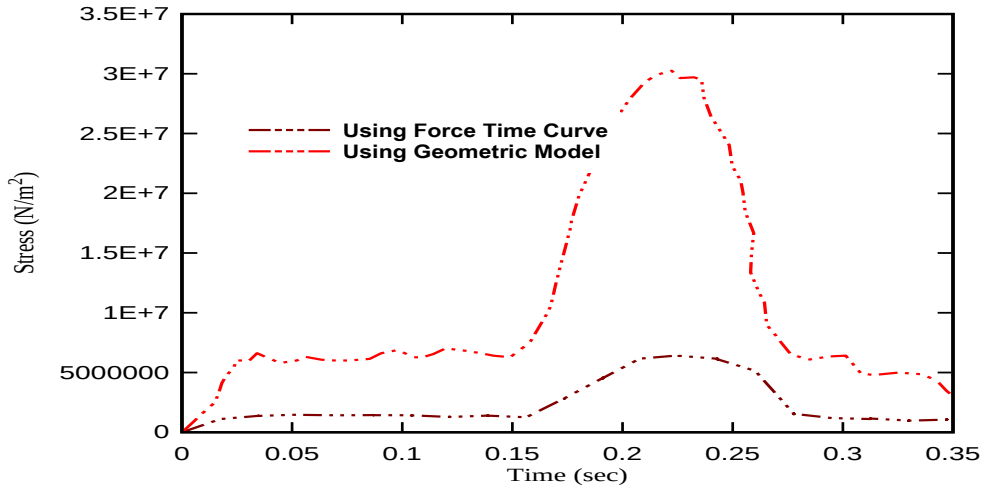

Fig. 6.26 Stress in single element at impact location of concrete body using different method

6.5 RESPONSE OF CONTAINMENT AGAINST TRIFURCATION APPROACH

A three-mile island reactor containment has been considered for trifurcation approach. In this approach the impact area is divided into three parts. The first part is for fuselage impact, second part is for the first set of engines and third part is for second set of engines, Fig. 6.27. the total contact area has been trifurcated in the following manner;

- A1: Area for Fuselage
- A2: Area for First set of engines
- A3: Area for Second set of engines

The shape of A1, A2 and A3 has been assumed in accordance with respective component of aircraft for which it has been designated, see Fig. 6.28. The reaction force of each component of aircraft has been applied on the corresponding area with respect to time. The total sum of A1, A2 and A3 has been found to be approximately 40 m^2. The corresponding reaction-time curve applicable for A1, A2 and A3 has been systematically segregated, see Fig. 6.29. The reaction force corresponding to the aircraft fuselage has been applied on A1 with respect to time. Similarly the reaction force thus obtained has been applied on the corresponding area (A2 and A3) with respect to time. The maximum deformation and stress contour in concrete has given in Fig. 6.30. The maximum deformation of 0.0143m and stress of 7.9 MPa are observed in concrete body. The maximum deformation of 0.0134m and stress of 32.4 MPa are observed in steel reinforcement bar, Fig. 6.31. Similarly, 0.0131m deformation and 59.8MPa stress was also found in inner steel liner, Fig. 6.32. Three different nodes were selected at A1, A2 and A3 regions to compare the results. The fuselage area (A1 area) has more deformation and stress which is obsereved from Figure 6.33 and 6.34. When the deformation and

stress along path B has been plotted for three approach, the deformation and stress predicted by the area trifurcation approach and the geometric model of the aircraft are comparatively high and in close agreement, Fig. 6.35 and 6.36. The trifurcation approach is therefore more accurate and realistic and hence can be employed to evaluate the response of the containment.

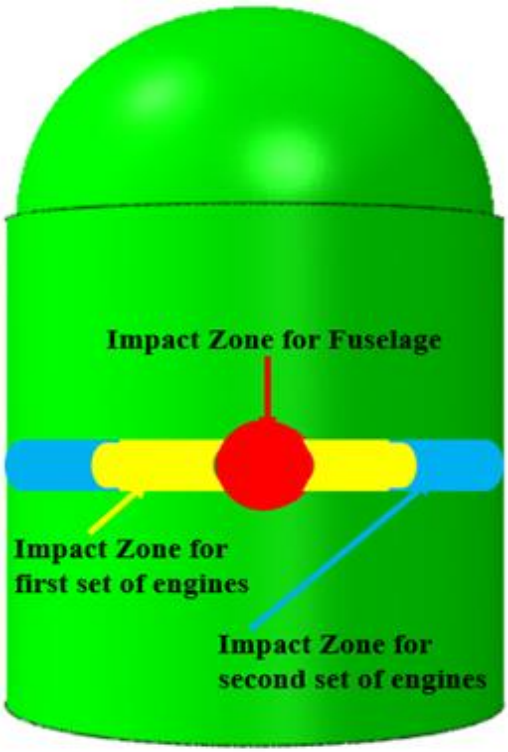

Fig. 6.27 Three-mile island containment with partition for trifurcation approach

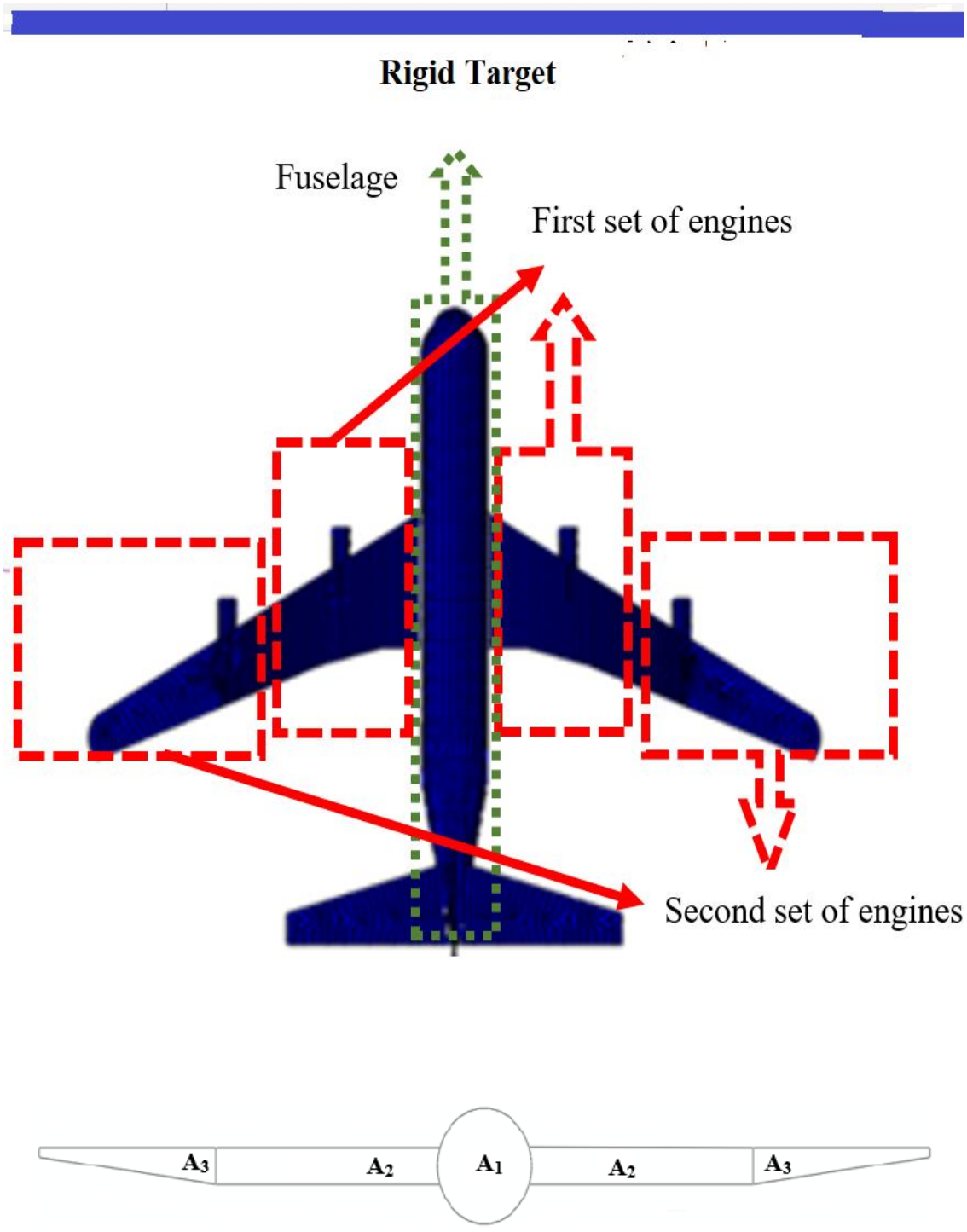

Fig. 6.28 Proposed area in trifurcation scheme

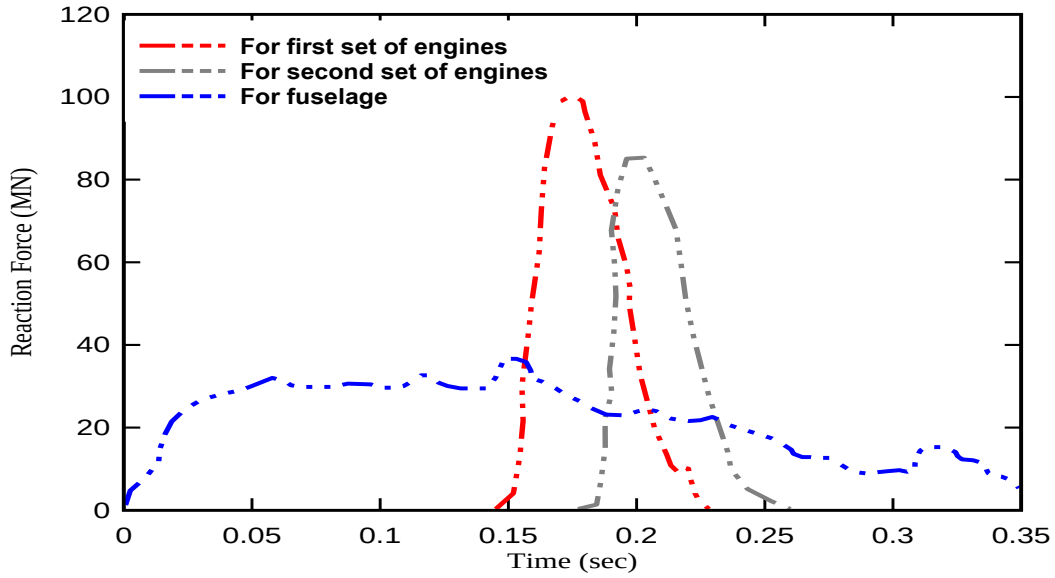

Fig. 6.29 Reaction force–time response curve with rigid target at three different zone

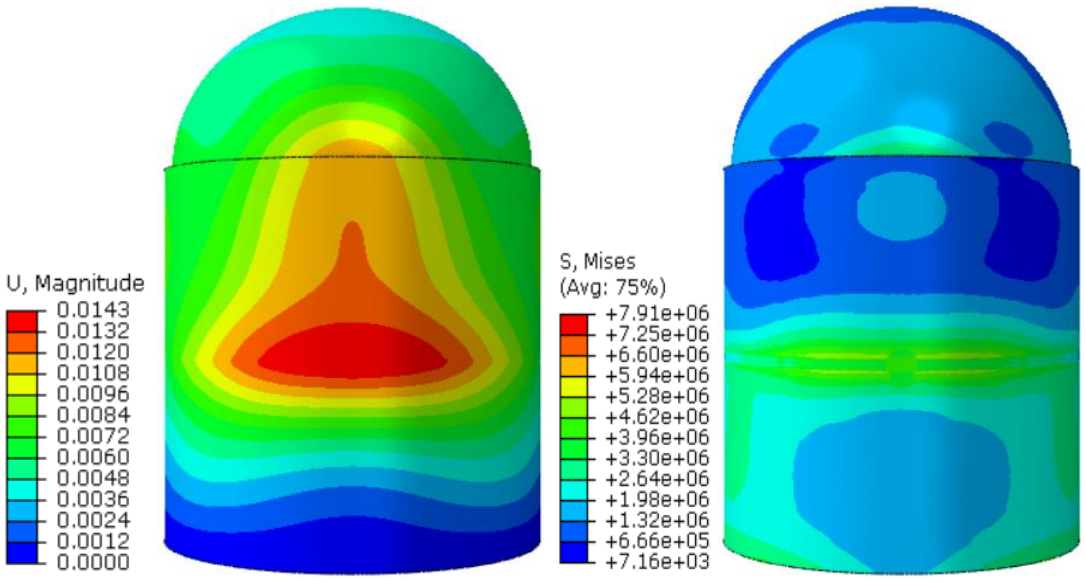

Fig. 6.30 Deformation and stress profile in concrete under trifurcation approach

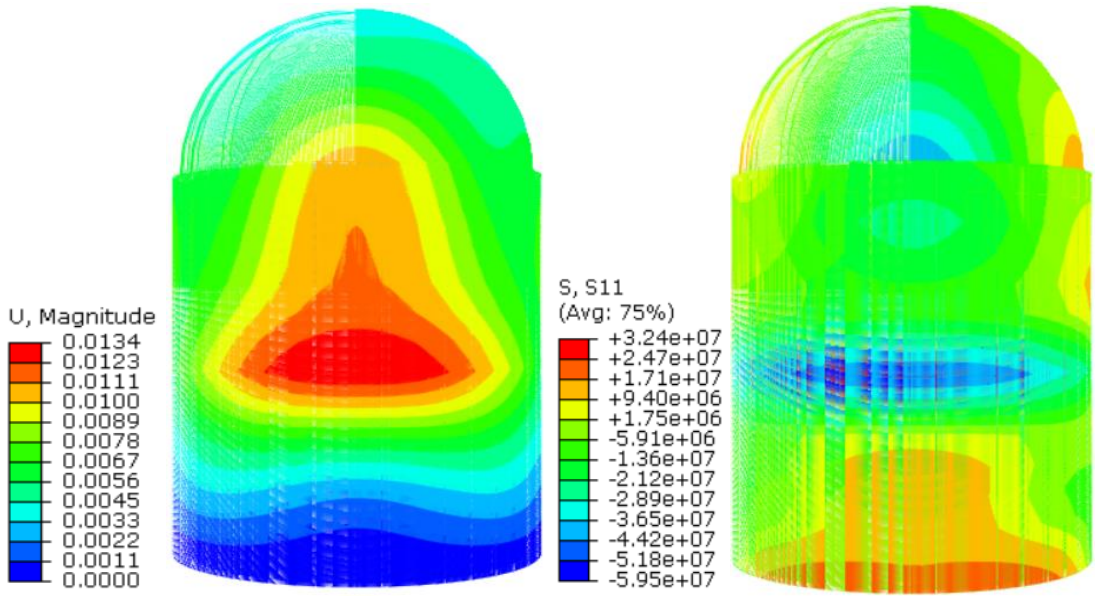

Fig. 6.31 Deformation and stress profile in steel reinforcement under trifurcation approach

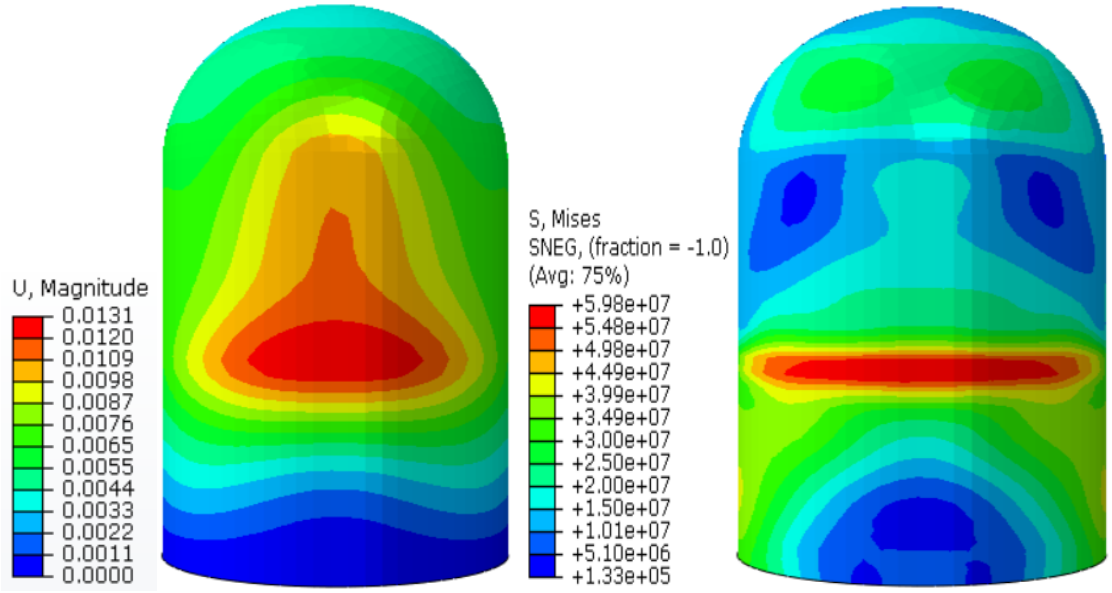

Fig. 6.32 Deformation and stress profile in inner steel liner under trifurcation approach

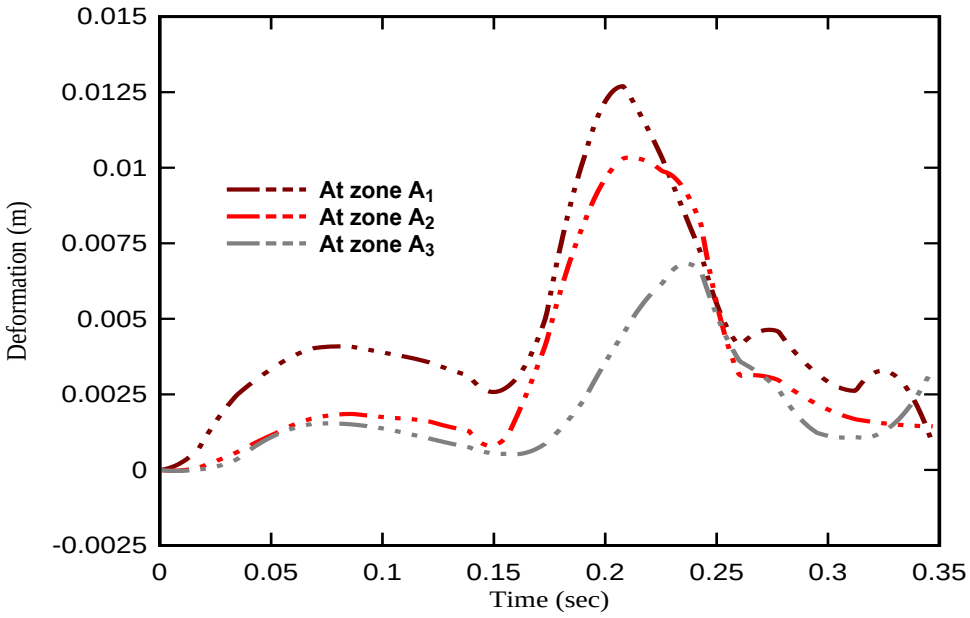

Fig. 6.33 Deformation in concrete element at zone A_1, A_2 and A_3 using trifurcation approach

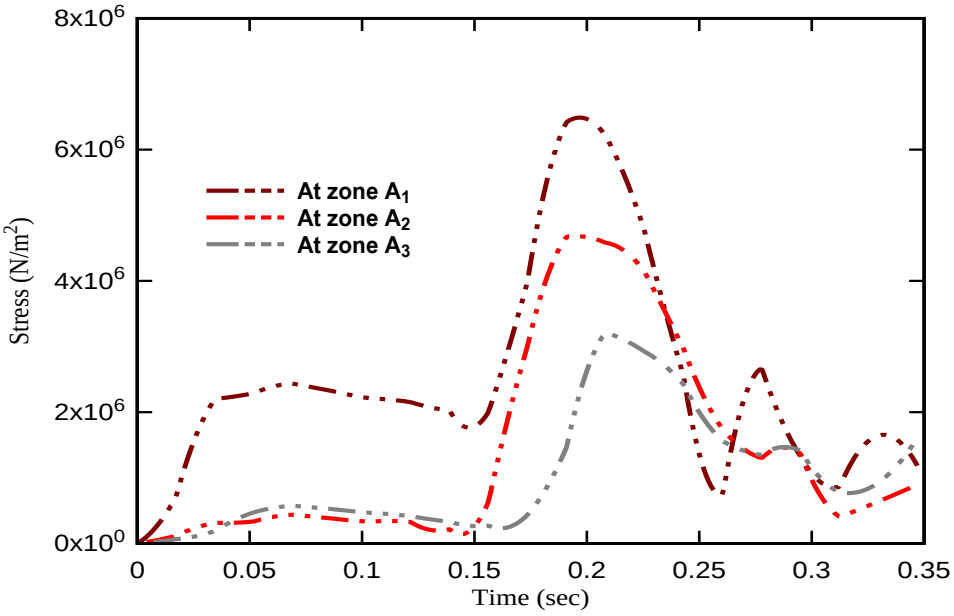

Fig. 6.34 Stress in concrete element at zone A_1, A_2 and A_3 using trifurcation approach

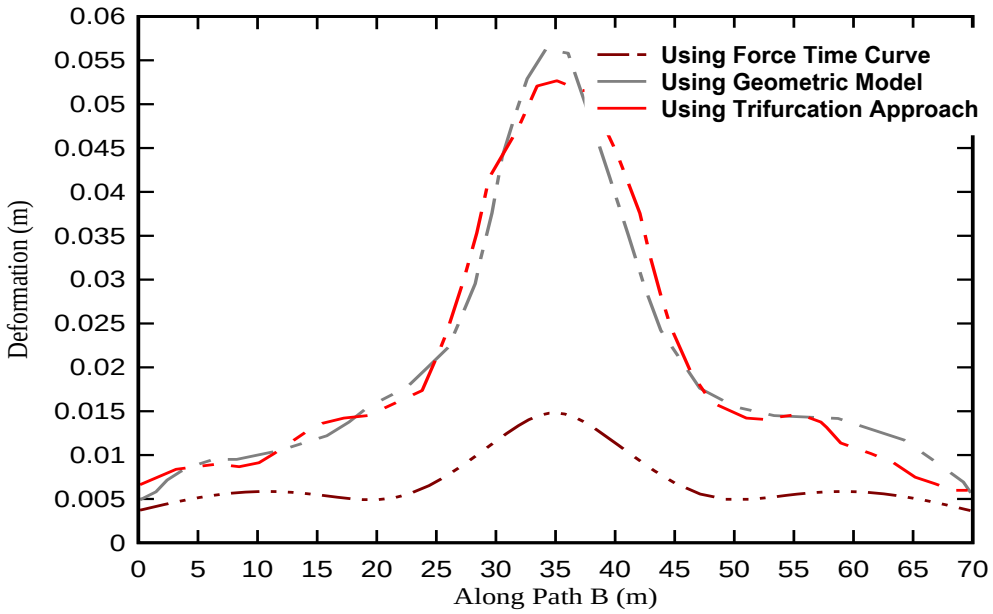

Fig. 6.35 Deformation in concrete along path-B using three different method

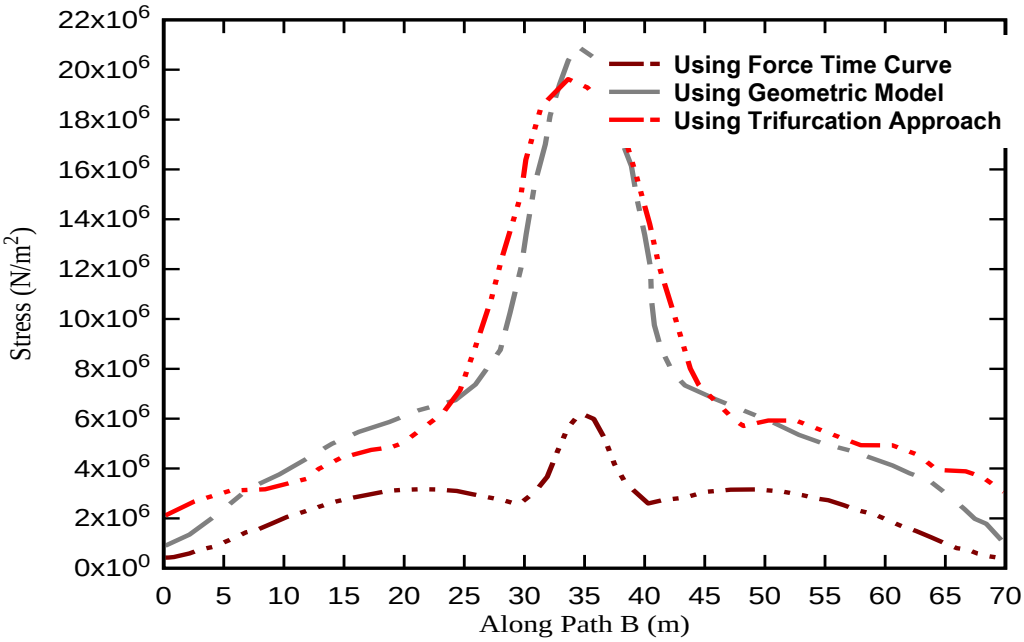

Fig. 6.36 Stress in concrete along path-B using three different method

6.6 SUMMARY

In the present chapter, the effect of target curvature, deformability and impact angle has been evaluated on the reaction-time curve. The responses of TMIR containment wall are calculated using different loading approach. From the present study the following major conclusion may be drawn:

- The curvature and deformability of the target are important parameters affecting the reaction-time response of aircraft. A decrement in the peak reaction force has been noticed with increase in target curvature.
- The reaction force developed by the deformable target is less in magnitude compare to the rigid target of similar shape and size.
- When the impact angle is normal to the rigid target, the maximum reaction force is observed.
- The formulating for reaction time response curve proposed by Riera 1968 should be modified considering all above parameters.
- The deformation response is found almost similar in nature for area trifurcation approach and geometric model approach. However, the geometric modeling of aircraft is very time consuming so the trifurcation approach is better solution scheme.